ECOLOGY LETTERS

Ecology Letters, (2012) **15**: 594–602 doi: 10.1111/j.1461-0248.2012.01777.x

LETTER

Mechanistic theory and modelling of complex food-web dynamics in Lake Constance

Alice Boit,[1]* Neo D. Martinez,[2] Richard J. Williams[3,4] and Ursula Gaedke[1]

Abstract

Mechanistic understanding of consumer-resource dynamics is critical to predicting the effects of global change on ecosystem structure, function and services. Such understanding is severely limited by mechanistic models' inability to reproduce the dynamics of multiple populations interacting in the field. We surpass this limitation here by extending general consumer-resource network theory to the complex dynamics of a specific ecosystem comprised by the seasonal biomass and production patterns in a pelagic food web of a large, well-studied lake. We parameterised our allometric trophic network model of 24 guilds and 107 feeding relationships using the lake's food web structure, initial spring biomasses and body-masses. Adding activity respiration, the detrital loop, minimal abiotic forcing, prey resistance and several empirically observed rates substantially increased the model's fit to the observed seasonal dynamics and the size-abundance distribution. This process illuminates a promising approach towards improving food-web theory and dynamic models of specific habitats.

Keywords

Allometric Trophic Network model, community ecology, food web, multi-trophic dynamics, seasonal plankton succession.

Ecology Letters (2012) **15**: 594–602

INTRODUCTION

Ecosystem functions and services critically depend on the dynamics of complex ecological communities. This dependence has long motivated a search for mechanistic explanations and predictions of community dynamics. However, the paucity of predictive community models suggests to many that such research on communities of interacting species has been largely misguided and scientifically unproductive (Lawton 1999; Ricklefs 2008). One exception to this criticism concerns food webs which represents a fruitful tradition of both empirical and theoretical network analysis (Lindeman 1942; MacArthur 1955; May 1973) and has led to ecological network theory that successfully predicts both general and specific system's structural properties (Williams & Martinez 2000, 2008; Dunne 2006; Allesina *et al.* 2008).

In contrast, progress predicting empirically observed population dynamics of many species feeding upon each other in the field has been more limited. Recent advances based on theoretical models such as the Allometric Trophic Network (ATN) model (Brose *et al.* 2006) integrate the above-mentioned structural theory with general metabolic consumer-resource theory of species' biomass gains from resource-based growth and loss to consumption and maintenance costs (Yodzis & Innes 1992) based on Rosenzweig-MacArthur models (Rosenzweig & MacArthur 1963). In addition to structural network parameters, this theory of dynamics requires species' body size and metabolic type as inputs. ATN models very generally model trophic interactions in a manner easily parameterised by allometric scaling rules which helps to develop basic theory of many dynamically interacting species. Other more applied models integrate locally focused hydrodynamic and biogeochemical models with biological models for managing dynamics of specific ecosystems (Baretta *et al.* 1995; Mooij *et al.* 2010). However, the focus on locally relevant biogeochemical cycles impedes the generalisation of these models to other ecosystem types (Omlin *et al.* 2001; Mieleitner & Reichert 2006), and the difficulties in deriving functional group parameters from distinct (laboratory) experiments often require a decrease in trophic resolution to a few groups. Other related models of many interacting species designed for fisheries management (Pauly *et al.* 2000) are constrained by mass-balance and fixed diet proportions. These constraints greatly increase the need for many site-specific parameters, significantly limit model generality and would likely prevent the rapid changes of species' populations needed to reproduce seasonal plankton dynamics.

To bridge this gap between generality and specificity and better address ecological complexity, we developed ATN models of intermediate generality with high trophic resolution and minimal abiotic forcing to test whether and how easily the ATN approach can reproduce observed time series of multiple interacting species. While ATN models are increasingly used for developing ecological theory (Brose 2010), they have only been tested against a limited range of temporal patterns and dynamic processes in natural ecosystems (Koen-Alonso & Yodzis 2005; Otto *et al.* 2007; Berlow *et al.* 2009). Broadening this range could enable ATN models and associated theory to help explain and predict multi-species dynamics by refining and corroborating modelled mechanisms. Such advances could then be integrated with site-specific abiotic sub-models to more effectively inform management of specific ecosystems subjected to human exploitation and global change. This research strategy directly

[1]*Department of Ecology and Ecosystem Modelling, Institute of Biochemistry and Biology, University of Potsdam, Am Neuen Palais 10, 14469 Potsdam, Germany*
[2]*Pacific Ecoinformatics and Computational Ecology Laboratory, 1604 McGee Avenue, Berkeley, CA 94703, USA*
[3]*Microsoft Research Ltd., 7 J. J. Thomson Avenue, Cambridge CB3 0FB, UK*
[4]*Quid Inc., 733 Front St, San Francisco, CA 94111, USA*
**Correspondence: E-mail: aboit@uni-potsdam.de*

addresses several calls to improve community ecology by extending theory to more types of predictions (McGill *et al.* 2007) and mapping fundamental traits such as body size onto biotic interactions (McGill *et al.* 2006) and food webs to forecast population dynamics and the effects of environmental change (Emmerson 2011). We do this here by applying ATN models to the seasonal dynamics of plankton organisms during the growing season when their trophic interactions largely govern system behaviour. This conceptually well-understood, classic example of complex ecological dynamics in the field (Sommer *et al.* 1986) is poorly reproduced by existing models for more than a few groups of organisms. The long-term dataset from well-studied, large and deep Lake Constance (LC) in central Europe presents an especially powerful opportunity to test our quantitative understanding with a highly resolved network of pelagic population dynamics.

This dataset describes seasonal patterns of succession among plankton from the spring bloom state dominated by relatively few, highly edible and fast growing algae that enable a late spring peak of generalist grazers which induce a clear water phase (CWP). Following the CWP, the community shifts to a more diverse state containing relatively many less edible algal species and several zooplankton guilds during the summer and autumn blooms. Five ATN models with progressively increasing parameter requirements and model complexity were constructed based on an aggregated food web of 20 plankton and 4 fish guilds (Table 1) found within the pelagic zone of LC. This

Table 1 The LC food web with size-related parameters and prey ranges in M0–M4

ID	Name	Description	Biomass*	Body mass†	x_i, r_i‡	FM§	Diet ID¶	Weak links**
Model M0								
0	DOC	Pool of dissolved organic carbon	500 000	n.a.	n.a.	n.a.	n.a.	n.a.
1	Alg1	Single-cell algae, ++††	5000	6.40E-05	1	a	n.a.	n.a.
2	Alg2	Large, single-cell algae or colonies, +	3000	2.56E-04	0.9	a	n.a.	n.a.
3	Alg3	Filamentous blue and green algae, –	30	3.20E-05	1.09***	a	n.a.	n.a.
4	Alg4	Diatoms, algal colonies, +	5000	1.28E-04	0.95	a	n.a.	n.a.
5	Alg5	Small, coccal algae, ++	5000	8.00E-06	1.38	a	n.a.	n.a.
6	APP	Autotrophic picoplankton, +	20	2.50E-07	2.4***	a	n.a.	n.a.
7	Bac	Heterotrophic bacteria	20 000	1.56E-08	1.04***	o	0	–
8	HNF	Heterotrophic nanoflagellates, B‡‡	1500	8.00E-06	0.43	f/i	6–7	–
9	Cil1	Small ciliates, **B**	30	2.56E-04	0.14	f	6–7	–
10	Cil2	Small ciliates, **B/H**	150	2.05E-03	0.18	i	1, 5–8	–
11	Cil3	Medium-size ciliates, **H**	2000	4.10E-03	0.15	f/i	1–2, 5, 8	2
12	Cil4	Medium-size ciliates, **H**	2000	8.19E-03	0.15	f	1, 5, 8	–
13	Cil5	Larger ciliates, **O**	300	6.55E-02	0.1	i	1–2, 4–5, 8–11	8
14	Rot1	Small rotifers, **B/H**	15	1.64E-02	0.13	f	1, 5–8	–
15	Rot2	Medium-size rotifers, **H**	15	3.28E-02	0.12	f	1–9	2–4, 9
16	Rot3	Large rotifers, **O**	50	6.55E-02	0.11	i	1–5, 8–9	2–4, 9
17	Asp	Large rotifers, **C**	50	6.55E-02	0.12	r	2–4, 8–16	–
18	Dap	Mostly cladocerans (daphnids), **H/O**	3000	8.39E+00	0.07	f	1–16	7, 11, 14–16
19	Cyc	Cyclopoid copepods, **O/C**	15 000	1.05E+00	0.07	r	1–5, 8–17	14–16
20	Lep	Large, carnivorous cladocerans, **C**	350	6.71E+01	0.04	r	17–18	–
21	Fish1	Fish larvae, **C**	5000	1.10E+06	0.07	r	14–19	–
22	Fish2	Juvenile fish, **C**	5000	4.40E+06	0.06	r	18–20	–
23	Fish3	Adult planktivorous fish, **C**	1000	3.52E+07	0.05	r	18–20	–
24	Fish4	Adult piscivorous fish, **C**	1000	7.04E+07	0.05	r	18–22	–
***Exceptions from allometric scaling in M1								
7	Bac	$x_i = 0.5$						
6	APP	$r_i = 0.6$						
***Exceptions from allometric scaling in M2–M4								
7	Bac	$x_i = 0.04$						
3	Alg3	$r_i = 0.4$						

Colours represent eight major functional groups: phytoplankton (1–6, green), heterotrophic bacteria (7, blue), HNF (8, orange), ciliates (9–13, magenta), rotifers (14–17, dark cyan), herbivorous Crustaceans (18, light red), carnivorous crustaceans (19–20) and fish (21–24, light blue).
*In (μgC m^{-3}).
†In (μgC per ind).
‡Mass-specific growth rate r and metabolic rate x of guild i (1/d, cf. Table S1).
§Feeding mode (a, autotroph; o, osmotroph; f, filter-feeder; i, interception feeder; r, raptorial/ambush feeder).
¶ID of resource guild.
**18 weak links deleted in M4.
††Edibility (++, well-edible; +, less edible; –, edible only for specialists).
‡‡General diet description (B, bacterivore; H, herbivore; C, carnivore; O, omnivore). The parameters values in M0 were kept in subsequent models, except for the three cases specified (Bac, APP and Alg3).
***Model-specific exceptions from allometric scaling (see above for details)

progression illuminates improvements needed for the ATN to reproduce LC's seasonal patterns and helps develop a strategy for achieving similar fit in other ecosystems.

METHODS

Lake Constance is a temperate, large (476 km^2), deep (mean depth = 101 m, max. depth = 252 m) and warm-monomictic lake, north of the European Alps, where plankton biomass and the growth regulating factors exhibit strong seasonality (Sommer *et al.* 1986). During winter and early spring, physical factors like irradiance, vertical mixing and temperature are the dominant mechanisms controlling species' abundances. After stratification is established from late spring onwards, trophic interactions, nutrient depletion and food quantity and quality control population dynamics (Gaedke *et al.* 2002; Tirok & Gaedke 2007b). Top-down control of phytoplankton peaks during the clear water phase (CWP), followed by alternating bottom-up and top-down control until late autumn when abiotic forcing becomes dominant again.

Measurements of physical and chemical parameters as well as plankton biomass and primary and bacterial production were conducted weekly during the growing season and approximately every 2 weeks in winter at different depths from 1987 to 1996. From 1987 to 1993, zooplankton production was calculated from mass-balanced flux-matrices for carbon derived from empirical measurements of standing stocks, bacterial and primary production, diet compositions, ingestion, respiration and growth rates. The matrices ensure that inputs into each compartment and the entire system equal all respective outputs considering changes in standing stocks as storage flows (Gaedke *et al.* 2002).

The complete LC food web contains 24 functional guilds and 107 feeding relationships (Table 1). For analysis and presentation purposes, we aggregated biomass and production data into 20 functional guilds of plankton (Table 1) which were further aggregated into eight major planktonic groups: phytoplankton (Phy), autotrophic picoplankton (APP), heterotrophic bacteria (Bac), heterotrophic nanoflagellates (HNF), ciliates (Cil), rotifers (Rot), herbivorous crustaceans (Herb. Cru), and carnivorous crustaceans (Carn. Cru).

We focused on the plankton community (20 guilds) in the top 20 m layer of the lake from which the empirical data were derived and which roughly corresponds to the epilimnion and the euphotic zone. The phytoplankton comprise six guilds varying e.g. in size, shape, edibility and nutrient demands including small, highly edible species (Alg1 and Alg5) and larger, less edible ones (Alg2–4) plus APP including cyanobacteria. The guild of heterotrophic bacteria (Bac) contains all bacterial strains other than autotrophic cyanobacteria. The zooplankton comprise 13 guilds: one guild of HNF, five guilds of small ciliated protozoan grazers (Cil1-5) and three guilds of medium-sized, metazoan grazers called rotifers (Rot1-3) that differ in respect to body mass, prey size rang, feeding modes and susceptibility to predation, one guild containing the larger rotifer *Asplanchna* spp. (Asp), one guild of predominantly herbivorous crustaceans including cladocerans such as daphnids and a calanoid copepod species (Dap), one guild of predominantly carnivorous crustaceans called cyclopoid copepods (Cyc), and one guild of large carnivorous crustaceans including *Leptodora* and *Bythotrephes* (Lep). The four fish guilds comprise fish larvae, juveniles, adult planktivorous and adult piscivorous fish (fish1–4).

We constructed an idealised time series for an average year (Fig. S2, using daphnids as an example), representing seasonal changes in biomass using approximately weekly biomass measurements and production estimates from 1987 to 1996 (Gaedke *et al.* 2002; de Castro & Gaedke 2008). Each year was divided into seven phases: 1, late winter; 2, early spring without stable stratification; 3, late spring with stable stratification; 4, CWP; 5, summer; 6, autumn; 7, early winter. We focused on phases 2–6 to exclude the abiotically governed phases 1 and 7. Given the annual variability in phase duration of up to several weeks, each datum was normalised to a time within a standard phase lasting the average number of days in that phase among the 10 years. The data was then averaged by interpolating a spline function among the normalised data cloud containing all 10 years of biomass data (Fig. S2). This minimises the influence of year-to-year weather events and emphasises more consistent and re-occurring ecological dynamics such as the spring bloom, the CWP, and summer and autumn blooms.

The ATN model is governed by a set of ordinary differential equations (ODE) originally formulated by Yodzis & Innes (1992) and extended to *n* species by Williams & Martinez 2004; Williams *et al.* 2007. We made several important modifications that add active metabolism, phytoplankton exudate, and dead particulate and dissolved organic carbon as detritus to the model. The ODEs for producers (1), consumers (2) and detritus (3) are:

$$\frac{dB_i}{dt'} = \overbrace{r_i \mathbf{B}_i G_i(\mathbf{B})(1-s_i)}^{\text{gain from producer growth}} - \sum_j \overbrace{\frac{x_i y_{ji} \mathbf{B}_j F_{ji}(\mathbf{B})}{e_{ji}}}^{\text{loss by consumers } j} \tag{1}$$

$$\frac{dB_i}{dt'} = \overbrace{-f_m x_i \mathbf{B}_i}^{\text{maintenance loss}} + \overbrace{f_a x_i \mathbf{B}_i \sum_j y_{ij} F_{ij}(\mathbf{B})}^{\text{gain from resources } j} - \sum_j \overbrace{\frac{x_i y_{ji} \mathbf{B}_j F_{ji}(\mathbf{B})}{e_{ji}}}^{\text{loss by consumers } j} - \overbrace{M(\mathbf{B})}^{\text{mortality}} \tag{2}$$

$$\frac{dD}{dt'} = \sum_i \sum_j \overbrace{\frac{x_i y_{ij} \mathbf{B}_i F_{ij}(\mathbf{B})}{e_{ij}}}^{\text{ingested resources } j \text{ by consumers } i} \overbrace{(1-e_{ij})}^{\text{egested}} + \sum_i \overbrace{r_i \mathbf{B}_i G_i(\mathbf{B}) s_i}^{\text{exudation by producers } i} - \sum_j \overbrace{\frac{x_j y_{ji} \mathbf{B}_j F_{ji}(\mathbf{B})}{e_{ji}}}^{\text{loss by detritivores } j}, \tag{3}$$

where B_i = biomass of guild i, r_i = intrinsic growth rate of producer i, $G_i(\mathbf{B})$ = the logistic growth function, s_i = fraction of exudation, x_i = mass specific metabolic rate of consumer i, y_{ij} = the maximum consumption rate of guild i feeding on j and e_{ji} = the assimilation efficiency describing the fraction of ingested biomass lost by egestion, f_m = the fraction of assimilated carbon respired by maintenance of basic bodily functions and f_a = the fraction of assimilated carbon used for production of consumers' biomass under activity ($1 - f_a$ is respired).

In eqn (1), we used the logistic growth function:

$$\mathrm{G_i}(\mathbf{B}) = 1 - \frac{\sum_{j=\text{producers}} c_{ij} \mathbf{B}_j}{K_\mathrm{s}} \tag{4}$$

with producer competition coefficients c_{ij} and a system-wide carrying capacity K_S that all autotrophs compete for. For simplicity and because these parameters cannot be derived from allometry alone, we assumed neutral competition effects for the basic models ($c_{ij} = 1$ for all algal guilds i, j) and set K_S to the maximum, averaged spring value

of the fast-growing reference producer (Alg1) multiplied by the number of phytoplankton guilds.

Mortality $M(\boldsymbol{B})$ is nonzero only for the four fish guilds which lacked seasonal estimates and are largely controlled by stocking and industrial fishing. We addressed these issues by adjusting $M(\boldsymbol{B})$ to force fish biomass to fit their long-term averages and therefore consume realistic amounts of the fish' prey (see Appendix S1 Supporting information, 'Top predator mortality' for details). $F_{ij}(\boldsymbol{B})$ in eqn (2) is the consumers' normalised functional response:

$$F_{ij}(\boldsymbol{B}) = \frac{\omega_{ij}\boldsymbol{B}_j^{q_{ij}}}{\boldsymbol{B}0_{ij}^{q_{ij}} + \sum_{k=consumers} d_{kj}p_{ik}\boldsymbol{B}_k\boldsymbol{B}0_{kj}^{q_{kj}} + \sum_{l=resources} \omega_{il}\boldsymbol{B}_l^{q_{il}}} \quad (5)$$

where ω_{ij} is the relative prey preference of consumer species i feeding on resource species j, $q_{ij} = 1.2$ which forms a relatively stable (Williams & Martinez 2004) Holling 1959 Type II functional response, $B0_{ij}$ = the concentration of resource species j at which consumer species i achieves half its maximum feeding rate on species j (Tables S1-S2), d_{kj} = the coefficient of feeding interference of consumer k with i while feeding on species j, p_{ik} = the fraction of resource species shared between species i and k. Interference is intraspecific when $k = i$ ($p_{ik} = 1$) and interspecific when $k \neq i$ ($0 \leq p_{ik} \leq 1$). We used the same set of d_{kj} (hereafter: prey resistance coefficients) to dynamically model prey resistance to increasing grazing pressure at high consumer biomass for a subset of feeding links in the model variants M2–M4. This set of d_{kj} (min = 0, mean = 0.07, max = 1, cf. Table S3) was manually calibrated because no empirical estimates for parameter values were available although prey resistance was observed for these feeding interactions (cf. Appendix S1).

Five ATN model variants (**M0**–**M4**) from very generalisable to more complex and specific to LC were built: The most basic, **M0,** is relatively standard (i.e. $f_m = f_a = 1$) with allometrically derived values of r_i or x_i for all guilds (Brose *et al.* 2006; Williams 2008) that are easily generalisable to many ecosystems. In **M1**, these rates were lowered for prokaryotes (Bac and APP) to fractions of the allometric estimates in accordance with more empirically based estimates for natural ecosystems in **M1** (cf. Appendix S1). **M1** also distinguishes the activity respiration of producing biomass ($f_a = 0.4$) from the metabolism that maintains biomass ($f_m = 0.1$). **M2** adds to **M1** prey resistance coefficients for 50% of all links to represent well known defence responses of plankton organisms subjected to varying predation pressure (cf. Appendix S1 and Table S3). **M3** adds to **M2** simple abiotic forcing representing seasonal changes in temperature, irradiance and decreasing K_s by nutrient depletion (cf. Appendix S1 and Fig. S1). **M4** eliminates from **M3** 18 links (17%, Table 1) known to be weak or not well verified by empirical data (cf. Table S1 for fuller model descriptions).

The modelled time series were recorded over 240 time steps translating to 8 months from March to October in the average year of the empirical time series (Fig. S2). A goodness-of-fit between the empirical and modelled time series for each phase was measured using the percentage (Bray–Curtis) similarity $Sim = 1 - 0.5\sum_{i=guilds} |pLC_i - pATN_i|$ with pLC_i and $pATN_i$ as the empirical and modelled guild fractions of guild i, respectively, calculated for the autotrophic to heterotrophic (A/H) biomass and production ratio, and for the relative biomass and production contributions to the plankton community. In addition, we measured goodness-of-fit by the following ratios of modelled quantities divided by those in the LC data: total biomass of all plankton guilds, total production of all plankton guilds, the total production to total biomass (P/B) ratio of the plankton community, and the slope of the size-abundance distribution among plankton (see Appendix S1). A ratio of 1 indicates a perfect match of the model to LC data. Furthermore, we used statistical variability measures to assess whether the modelled time series stayed within LC's natural variability (cf. Appendix S1 and Fig. S2).

RESULTS

The most consistently reproduced empirical pattern is the slope of LC's size-abundance distribution which is matched well by all models in most phases (Table S4). All models except the most basic M0 also reproduce LC's high-level biomass and production patterns measured by the A/H ratios. Extinctions (i.e. the permanent decline to very low densities) do not occur despite the considerable prey range overlap of many consumer guilds (Fig. 1).

More specifically, M0 explains one third of the seasonal biomass variability of the 20 guilds (avg. sim. = 0.33; eight-group avg. sim. = 0.54, Fig. 2 and Table S4) and matches the biomass A/H of LC surprisingly well (avg. sim. = 0.91) at least partly due to the phytoplankton community carrying capacity, K_s, maintaining realistic amounts of producer biomass (Figs S3 and S4). Still, M0 overestimates APP's contribution to phytoplankton by overestimating APP's growth rate. This causes APP to suppress eukaryotic phytoplankton biomass which M0 underestimates by up to 50% (Figs S3 and S4). Production A/H unrealistically falls below 50 : 50 in three phases and

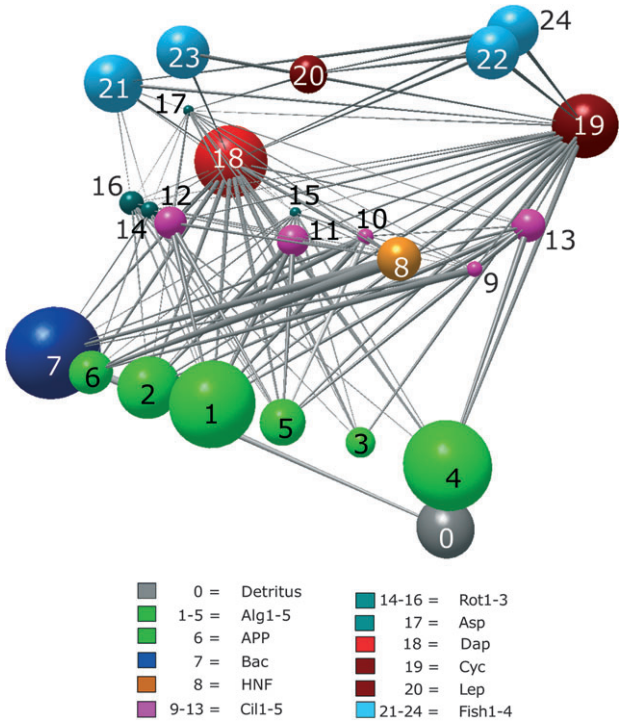

Figure 1 The LC food web in Network 3D (Yoon *et al.* 2004; see Table 1 for details). Nodes except detritus are scaled with biomasses and links with the carbon flow averaged over the seasonal phases 2–6. The vertical axis indicates the trophic position. The guild Bac contains heterotrophic bacteria. The six phytoplankton guilds are: APP (autotrophic picoplankton including cyanobacteria) and Alg1-5 (eukaryotic). The 13 zooplankton guilds are: heterotrophic nanoflagellates (HNF), Cil1-5 (ciliates), Rot1-3 (rotifers), Asp (the large, predatory rotifer genus *Asplanchna*), Dap (predominantly herbivorous cladocerans like daphnids), Cyc (predominantly carnivorous cyclopoid copepods) and Lep (large carnivorous cladocerans). Fish guilds are Fish1-4 (zooplanktivorous and piscivorous).

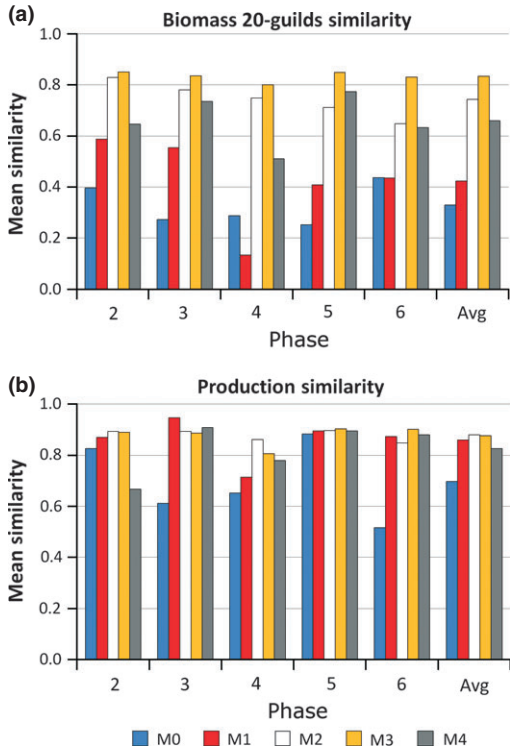

Figure 2 Summary of M0-M4 models' fit to relative biomass and relative production within each temporal phase. Phases are 2, early spring; 3, late spring; 4, CWP; 5, summer; 6, autumn. Mean percentage similarity between modelled and empirical biomass (a) and production (b) percentages in each phase and averaged across seasons.

heterotrophic relative production is overestimated by up to 50%, (Figs S3 and S5) resulting in a relatively low production similarity (avg. sim. = 0.70). Small organisms with unrealistically high metabolic rates like Bac, APP and HNF cause the model to overestimate total production resulting in a 68% higher total P/B.

M1 corrects for the well-known allometric overestimation of prokaryote metabolic rates and separates activity from maintenance metabolism for heterotrophs. Compared with M0, M1 yields more similar seasonal variability in relative biomass (avg. sim. = 0.42, eight-group avg. sim. = 0.69) and production (avg. sim. = 0.86). M1 also yields a realistic production A/H (avg. sim. = 0.95) as well as a very similar biomass A/H ratio (avg. sim. = 0.84). Mainly due to the accumulation of bacterial and phytoplankton biomass, the model overestimates total biomass (57% higher on avg.) more than total production (37% higher on avg.) so that in contrast to M0, total P/B is slightly underestimated (avg. ratio = 0.77).

Compared with M1, M2's inclusion of prey defense substantially improves the fit to seasonal variability in relative biomass (avg. sim. = 0.74, eight-group avg. sim. = 0.78) and leaves seasonal production similarity only slightly improved (avg. sim. = 0.88). The more LC-specific M2 achieves an accurately timed CWP induced by the combined grazing pressure of ciliates, rotifers and omnivorous daphnids. The daphnids develop a sufficient density (Figs S3–S4) to keep phytoplankton and smaller grazers under top-down control and prevent ciliates and phytoplankton from developing predator-prey cycles. As observed during the CWP, phytoplankton achieves its least relative biomass and production while consumers and bacteria achieve their highest relative production. The critically important timing of daphnids's dominance among the grazers for the onset and intensity of the CWP depends on the amount of prey resistance applied to the links of ciliates, rotifers and cyclopides who share daphnids's phytoplankton and bacterial resources. After 20–30 days in early summer (phase 5), the CWP terminates due to the increase of well-fed carnivorous second and third level predators (*Leptodora* & *Bythotrephes*, fishes) and scarce phytoplankton reducing daphnids below their CWP maxima for the rest of summer and autumn. M2's A/H biomass ratio is very similar to LC (avg. sim. = 0.92). However, the lack of dampening by M3's abiotic forcing causes M2 to develop predator-prey cycles after the CWP between small grazers and phytoplankton which reduces M2′s relative biomass similarity towards autumn. M2 overestimates total biomass as much as total production (about 75% on avg.) due to the lack of abiotic forcing. Still, total P/B falls into a realistic range (model/data ratio = 1.06).

M3's simple addition of abiotic forcing results in our best fit model among virtually all average fitness measures including relative seasonal biomass (20-guilds avg. sim. = 0.83, eight-group avg. sim. = 0.90) and production (avg. sim. = 0.88) similarity (Fig. 2 and Table S4). M3's improved fit over M2′s is most prominent after the CWP when less-edible algae guilds accurately gain biomass relative to more edible ones during the summer (Fig. 3). As seen in LC, this results in the maximal evenness of the communities' biomass distribution during the annual succession as corroborated by M3's consistently similar biomass for all 20 plankton groups within each phase (0.80–0.85) and very close match to total biomass (avg. ratio = 0.94), and average A/H biomass ratio (M3; 36 : 64 vs. LC; 35 : 65). The high biomass similarity is relatively insensitive to using biweekly or weekly averages instead of the phase means (Table S5a). This insensitivity confirms that the modelled dynamics stay within the bounds of LC's within-phase variability.

Looking more closely at production (Fig. 4), M3's average A/H production ratio (74 : 26) is very similar to that in LC (68 : 32) with a close match for total production (avg. ratio = 0.95). Absolute primary production is highest in spring, enabling the build-up of zooplankton's biomass which subsequently triggers the CWP during which the relative share of phytoplankton production is lowest due to grazing whereas its production to biomass ratio (P/B) is maximal. More generally, M3′s average total P/B ratio is realistic overall (avg. ratio = 1.04), but underestimated in early spring (35–50% below LC) due to phytoplankton reaching its capacity too quickly and being slightly overestimated in summer and autumn presumably due to the lack of explicit nutrient limitation (51–60% above LC; Fig. 4d, e). Ciliate guilds are systematically underestimated whereas rotifer guilds are overestimated (Figs 3b–d and 4c). These guilds together account for less than 5% of the biomass and production in LC. The size-abundance distribution of M3 fits very well over the full size range in LC including the characteristic seasonal development of this distribution from a slope < -1 in spring to a slope > -1 during the CWP when larger organisms (daphnids) dominate the community (Fig. 5).

Removing the weakest links from M3 in the final model M4 reduces its fit to biomass similarity (avg. sim. = 0.66, eight-group avg. sim. = 0.72) because M4 fails to reproduce the CWP. This is due to daphnids' reduced peak density in the absence of weak, but dynamically important links to daphnids' resources. M4′s underestimation of herbivorous and carnivorous production among crustaceans causes the model to underestimate total biomass and total production by on average 30% and 50%, respectively. However, M4

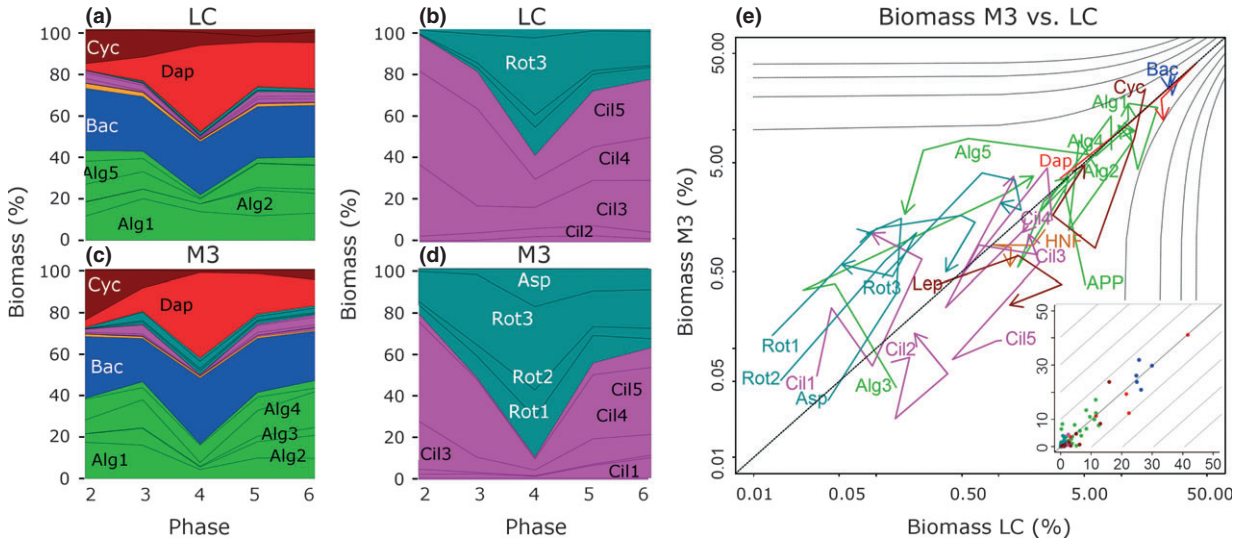

Figure 3 (a) Comparison of relative biomass observed in LC and (c) modelled by M3 of 20 plankton guilds from early spring to autumn. (b) Magnified relative biomass distribution of the highly diverse, but low-biomass guilds Cil and Rot in LC and (d) in M3. (e) Direct comparison of relative biomass contributions between M3 and LC. Arrows connect phases 2–6 (inset is linearly scaled). Dashed line at $x = y$ indicates perfect fit. Each reference line above (below) the $x = y$ line indicates a 10% increase (decrease) of the model in reference to total biomass. Colour scheme same as Fig. 1.

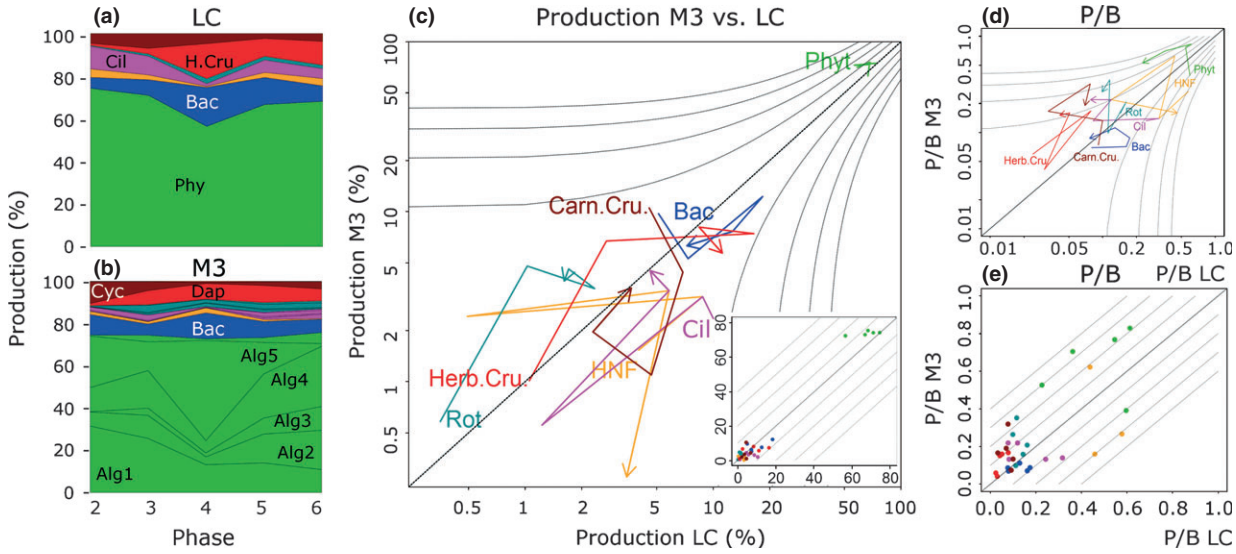

Figure 4 (a) Comparison of relative production (per day) of seven major plankton groups Phy, phytoplankton including APP; Bac, heterotrophic bacteria; HNF, Cil, ciliates; Rot, Rotifers; Herb. Cru, herbivorous crustaceans; Carn. Cru, carnivorous crustaceans observed in LC and (b) modelled by M3 from early spring to autumn. (c) Direct comparison of relative production contributions between M3 and LC. Arrows connect phases 2–6 (inset is linearly scaled). Dashed line at $x = y$ indicates perfect fit. Each reference line above (below) the $x = y$ line indicates a 10% increase (decrease) of the model in reference to total production. (d, e) P/B ratios are compared using log (d) and linear (e) scales. Colour scheme same as Fig. 1.

still has high similarity to production variability (avg. sim. = 0.83) which is less affected by the missing links.

DISCUSSION

Advances in predator-prey theory have achieved mechanistic understanding and accuracy of two-species population dynamics within chemostats using Rosenzweig-MacArthur models (Shertzer *et al.* 2002). Food-web theory has progressed from revealing patterns in food-web structure (Martinez 1993; Dunne 2006) to the discovery of successfully predictive rules behind that structure (Williams & Martinez 2000, 2008; Cattin *et al.* 2004; Allesina *et al.* 2008). Integrating this structural food-web theory with a relatively simple, scalable and easily parameterised versions of advanced Rosenzweig-MacArthur models based on bioenergetic consumer-resource equations (Yodzis & Innes 1992) improved explorations of complex food-web dynamics in model ecosystems (Brose *et al.* 2006; Martinez *et al.* 2006). Such studies help explain dynamic persistence in complex ecosystems (Otto *et al.* 2007) and successfully predict empirical predator-prey body-size ratios (Brose *et al.* 2006), and the

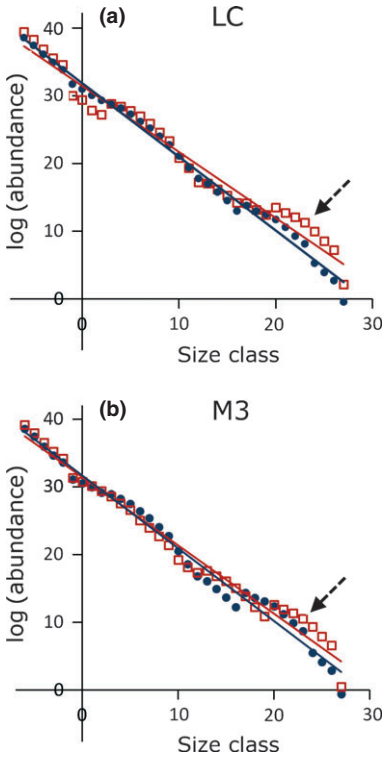

Figure 5 Log abundance (number of individuals per m^3) per size class (log body mass in pgC m^{-3}) in the plankton community during early spring (blue dots) and the CWP (red squares) as observed in LC (a) and modelled in M3 (b). Seasonal patterns like the daphnids' peak (dashed arrows) were reproduced by M3. Spring values for the slope are: −1.09 (LC) and −1.08 (M3), which becomes shallower during the CWP: −0.98 (LC) and −1.00 (M3) due to the high (low) abundances of daphnids (phytoplankton). This pattern is also reflected in the decrease of the regression coefficient R^2 during the CWP (from R^2 = 0.99–0.97 in LC, and from R^2 = 0.99–0.98 in M3).

dynamic effects of removing species in field experiments (Berlow *et al.* 2009). Here, we extend the empirical tests of theory beyond simple systems with highly controlled environmental conditions and find that the general theory formalised as ATN model tests well against multi-species time series in the field when including activity respiration and the detrital loop. This advances ecology by developing and testing community theory in new ways and also by showing that a complex and trophically highly resolved data set like that from LC can be surprisingly accurately modelled by employing mechanistic theory.

The close and relatively straightforward fit to LC data found in this test combined with the earlier advances help to build a theoretical core for community ecology based on first principles asserting central roles for food and metabolism in determining population dynamics and species' interactions. Discovering such a core was thought unlikely or impossible at the level of multi-species communities and more likely at population and macro-ecological levels (Lawton 1999). Our results challenge this view by suggesting a more scientifically optimistic outlook for understanding and predicting the dynamics of multi-species communities.

The modifications needed to better reproduce LC data illuminate how to surpass previous limitations and apply community network theory to the complex behaviours of specific systems. Such guidance is needed because time series of interacting plankton can be fitted using disparate modeling approaches (Friedrichs *et al.* 2007). A key foundation of our application is the remarkable persistence of allometrically scaled nonlinear bioenergetic models of realistically structured ecological networks (Brose *et al.* 2006; Brose 2008; Gross *et al.* 2009). This enables all guilds to persist indefinitely among all our models including the very basic M0 model. However, M0 greatly overestimates heterotrophic production and explains only a third of seasonal biomass variability among 20 plankton guilds. Still, M0 explains over a half of such variability among the eight more aggregated plankton groups. These more realistic contributions of groups, especially with respect to the bacteria, are enabled by a relatively simple addition of the detrital loop to the ATN framework. Given that the ratio between bacterial and primary production characterises many ecosystem types, more sophisticated modelling of the detrital loop that distinguishes refractory from labile detritus with differing decomposition rates may be required for forest food webs where, unlike LC, most plant production directly enters the detrital loop.

Extending ATN theory and models by separating the metabolic costs into maintenance and activity respiration was particularly effective for achieving realistic energetics. Compared with M0 which kept the earlier non-differentiated metabolism (Yodzis & Innes 1992), the separation of activity metabolism in M1 reduces maintenance costs to a size-dependent fraction of biomass per day and increases activity costs to 60% of assimilation so that at most 30% of consumption is converted into consumer's biomass (Gaedke & Straile 1994). This more realistic transfer efficiency is also reflected in the accurately reproduced value and seasonal changes of the slope of the size-abundance distribution maintaining an approximately even biomass distribution along the size gradient (Fig. 5) as typical of plankton systems (Sheldon *et al.* 1972). M1′s distinction of active and maintenance metabolism in combination with the lowered metabolic rates for prokaryotes improved the average biomass and production similarity from 0.33 to 0.42 and 0.70 to 0.86, respectively, and achieved realistic energetics reflected by a high production similarity (>0.82) in all subsequent models.

M1 lowered metabolic rates for three guilds known to deviate from allometric rules: the prokaryotic guilds bacteria and APP (M1), and the thermophilic Alg3 (M2). There is strong evidence that lowering metabolic rates for prokaryotes may also better reproduce natural production rates in other ecosystems (e.g. soil systems; cf. Appendix S1). In contrast with this improvement, reducing growth of the thermophilic algae Alg3 as in M2 did not further improve production similarity because the phytoplankton's total production is constrained by a common system capacity. It did, however, improve the biomass fit because this relatively inedible guild's growth occurs primarily in LC's summer.

Improving fit to the energy flow and resulting production patterns largely depends on revising system energetics (M0 vs. M1). However, adding prey resistance (M2), abiotic forcing (M3), or changing the topology (M4) impacts biomass patterns much more strongly. Adding prey resistance improves the fit for relative biomass from M1's values (avg. sim. = 0.42) to 0.74 in M2 largely by effectively preventing predator-prey cycles between phytoplankton and small grazers observed in M1, but not in LC. Non-zero values for prey resistance parameters (min = 0, mean = 0.07, max = 1) were assigned to 53 of the 107 links in the LC web representing feeding links concerning prey such as algae and daphnid populations well known to respond to increasing grazing pressure by becoming more resistant to consumption. Although

different density-dependent prey resistance to predator mechanisms are common in nature and appear dynamically important in LC (Tirok & Gaedke 2007a), they are rarely included in more complex community models. However, prey resistance is an important component of successful modelling of more isolated predator prey systems (Yoshida *et al.* 2007; Jones *et al.* 2009). The importance of prey resistance to modelling LC dynamics suggests that a more mechanistic inclusion of prey resistance as used here by modelling dynamic traits influencing prey edibility and consumer selectivity of species constrained by ecological trade-offs and variable predation pressure (Tirok & Gaedke 2010; Tirok *et al.* 2011) may improve the realism of model behaviour.

Adding abiotic forcing in M3 further increased the relative biomass similarity from 0.74 (M2) to 0.83 and resulted in 36% autotrophic, 25% bacterial and 39% other heterotrophic biomass, and 70% autotrophic, 10% bacterial and 20% other heterotrophic production overall. These contributions are similar to other pelagic systems (Cole *et al.* 1988) and further demonstrate that it is possible to reproduce generally observed, complex ecological dynamics with a relatively simple, but energetically realistic ATN model.

Despite the overall good fit of M3, the simplicity of its abiotic forcing led to the underestimation of total P/B and production in spring caused by phytoplankton quickly approaching its capacity with decreasing growth rates [enforced by eqn (1)] until sufficient grazing pressure had developed in late spring. M3 then slightly overestimated phytoplankton production in summer and autumn due to the lack of explicit nutrient limitation.

M4's high production similarity and rather low biomass similarity demonstrates the insensitivity and sensitivity of the LC-specific production and biomass patterns, respectively, to changes in food-web topology. The insensitivity of production similarity appears due to compensatory effects maintained by energy being channelled through other, functionally similar links. However, the decreased resource availability for daphnids at critical times prevented them from increasing sufficiently to induce the CWP. Although striking, the CWP occurs in only one of the five modelled phases and is less pronounced in LC during certain years. This limited prevalence of the CWP suggests that it is a fragile event that can easily be disrupted by topological changes that remove resource links from the keystone consumers that induce the CWP. Moreover, the keystone effect of daphnids during the CWP in lakes is supported by allometry-independent life history attributes of this guild and the competing cyclopides (Lampert & Schober 1978) which the ATN model does not account for (cf. Appendix S1). Such guild-specific traits may contribute to the M3's sensitivity to the deletion of weak links. These traits may be included for higher system-specific accuracy at the cost of higher model complexity and reduced generality.

In summary, our modified ATN model successfully reproduced the well-resolved seasonal plankton succession in LC, including the highly resolved upper trophic levels during the growing season. This addresses the observation that, 'no comprehensive lake ecosystem model has successfully managed to simulate, with complete accuracy, the succession dynamics of algae and zooplankton' (Gal *et al.* 2009) by closely and mechanistically fitting one of the most complex time series of multi-species dynamics available. Improving the ATN model with more realistic energetics and detrital dynamics integrates the successful site specificity of ecosystem models developed for management purposes with the more mechanistic modelling of two or three trophically interacting species in the laboratory, using a more general, scalable and easily parameterised approach.

This success suggests the following general strategy to modify and apply basic ATN theory to natural ecosystems: (1) Include topological and allometric information at the desired resolution of functional groups, (2) close the detrital loop, (3) correct for parameters poorly estimated by allometry, (4) separate activity from maintenance metabolism, (5) include essential aspects of abiotic forcing affecting the metabolic rates, (6) modify interaction strengths by including information on prey resistance, predator interference or other measures calibrated by observations when available.

Further extension of ATN models such as integrating stoichiometry, more sophisticated biogeochemical dynamics, and other indicators of food quality may powerfully advance food-web theory and its application. Predicting dynamics with higher accuracy in a distinct period at a specific location may be achieved by integrating the ATN model with a site-specific abiotic sub-model at the cost of generality. However, even without such further extensions, the advances achieved here help increase scientists' ability to better address important effects of global change, such as biodiversity loss and climate disruption on the structure, dynamics and services of ecosystems on which humans critically depend.

ACKNOWLEDGEMENTS

We thank Marcel Holyoak and three anonymous referees for the valuable comments on this manuscript, and Francisco de Castro for support in compiling the LC data set. This work was funded by Microsoft Research, the Heinrich Böll Foundation Berlin, the USA National Science Foundation, and benefitted from the EU Project FEMMES. Data acquisition was mostly performed within the Special Collaborative Program (SFB) 248 'Cycling of Matter in Lake Constance' supported by the German Research Foundation (DFG).

AUTHORSHIP

AB, NDM, RJW and UG designed research; AB performed research and analysed data; RJW contributed new analytic tools; and AB, NDM and UG wrote the article.

CONFLICTS OF INTEREST

The authors declare no conflict of interest.

REFERENCES

Allesina, S., Alonso, D. & Pascual, M. (2008). A general model for food web structure. *Science*, 320, 658–661.

Baretta, J.W., Ebenhöh, W. & Ruardij, P. (1995). The European-Regional-Seas-Ecosystem-Model, a complex marine ecosystem model. *Neth. J. Sea Res.*, 33, 233–246.

Berlow, E.L., Dunne, J.A., Martinez, N.D., Stark, P.B., Williams, R.J. & Brose, U. (2009). Simple prediction of interaction strengths in complex food webs. *Proc. Nat. Acad. Sci. USA*, 106, 187–191.

Brose, U. (2008). Complex food webs prevent competitive exclusion among producer species. *Proc. R. Soc. B: Biol. Sci.*, 275, 2507–2514.

Brose, U. (2010). Body-mass constraints on foraging behaviour determine population and food-web dynamics. *Funct. Ecol.*, 24, 28–34.

Brose, U., Williams, R.J. & Martinez, N.D. (2006). Allometric scaling enhances stability in complex food webs. *Ecol. Lett.*, 9, 1228–1236.

de Castro, F. & Gaedke, U. (2008). The metabolism of lake plankton does not support the metabolic theory of ecology. *Oikos*, 117, 1218–1226.

Cattin, M.F., Bersier, L.F., Banasek-Richter, C., Baltensperger, R. & Gabriel, J.P. (2004). Phylogenetic constraints and adaptation explain food-web structure. *Nature*, 427, 835–839.

Cole, J.J., Findlay, S. & Pace, M.L. (1988). Bacterial production in fresh and saltwater ecosystems – a cross-system overview. *Mar. Ecol. Prog. Ser.*, 43, 1–10.

Dunne, J.A.. (2006). The network structure of food webs. In: *Ecological Networks: Linking Structure to Dynamics in Food Webs* (eds Dunne, J.A. & Pascual, M.). Oxford University Press, Oxford, pp. 27–86.

Emmerson, M.C. (2011). The predictive science of community ecology. *J. Anim. Ecol.*, 80, 1111–1114.

Friedrichs, M.A.M., Dusenberry, J.A., Anderson, L.A., Armstrong, R.A., Chai, F., Christian, J.R. *et al.* (2007). Assessment of skill and portability in regional marine biogeochemical models: role of multiple planktonic groups. *J. Geophys. Res.*, 112, 1–22.

Gaedke, U. & Straile, D. (1994). Seasonal changes of trophic transfer efficiencies in a plankton food web derived from biomass size distributions and network analysis. *Ecol. Model.*, 75/76, 435–445.

Gaedke, U., Hochstädter, S. & Straile, D. (2002). Interplay between energy limitation and nutritional deficiency: empirical data and food web models. *Ecol. Monogr.*, 72, 251–270.

Gal, G., Hipsey, M.R., Parparov, A., Wagner, U., Makler, V. & Zohary, T. (2009). Implementation of ecological modeling as an effective management and investigation tool: Lake Kinneret as a case study. *Ecol. Model.*, 220, 1697–1718.

Gross, T., Rudolf, L., Levin, S.A. & Dieckmann, U. (2009). Generalized models reveal stabilizing factors in food webs. *Science*, 325, 747–750.

Holling, C.S. (1959). Some characteristics of simple types of predation and parasitism. *Can. Entomol.*, 91, 385–398.

Jones, L.E., Becks, L., Ellner, S.P., Hairston, N.G., Yoshida, T. & Fussmann, G.F. (2009). Rapid contemporary evolution and clonal food web dynamics. *Philos. Trans. R. Soc. B: Biol. Sci.*, 364, 1579–1591.

Koen-Alonso, M. & Yodzis, P. (2005). Multispecies modelling of some components of the marine community of northern and central Patagonia, Argentina. *Can. J. Fish. Aquat. Sci.*, 62, 1490–1512.

Lampert, W. & Schober, U. (1978). The regular pattern of spring algal bloom and extremely clear water in Lake Constance as a result of climatic conditions and planktonic interactions. *Arch. Hydrobiol.*, 82, 364–386.

Lawton, J.H. (1999). Are there general laws in ecology? *Oikos*, 84, 177–192.

Lindeman, R.L. (1942). The trophic-dynamic aspect of ecology. *Ecology*, 23, 399–418.

MacArthur, R. (1955). Fluctuations of animal populations, and a measure of community stability. *Ecology*, 36, 533–536.

Martinez, N.D. (1993). Effect of scale on food web structure. *Science*, 260, 1412.

Martinez, N.D., Williams, R.J. & Dunne, J.A.. (2006). Diversity, complexity, and persistence in large model ecosystems. in: *Ecological Networks: Linking Structure to Dynamics in Food Webs* (eds Pascual, M. & Dunne, J.A.). Oxford University Press, Oxford, pp. 163–185.

May, R.M. (1973). Stability and complexity in model ecosystems. *Monogr. Popul. Biol.*, 6, 1–235.

McGill, B.J., Enquist, B.J., Weiher, E. & Westoby, M. (2006). Rebuilding community ecology from functional traits. *Trends Ecol. Evol.*, 21, 178–185.

McGill, B.J., Etienne, R.S., Gray, J.S., Alonso, D., Anderson, M.J., Benecha, H.K. *et al.* (2007). Species abundance distributions: moving beyond single prediction theories to integration within an ecological framework. *Ecol. Lett.*, 10, 995–1015.

Mieleitner, J. & Reichert, P. (2006). Analysis of the transferability of a biogeochemical lake model to lakes of different trophic state. *Ecol. Model.*, 194, 49–61.

Mooij, W.M., Trolle, D., Jeppesen, E., Arhonditsis, G., Belolipetsky, P.V., Chitamwebwa, D.B.R. *et al.* (2010). Challenges and opportunities for integrating lake ecosystem modelling approaches. *Aquat. Ecol.*, 44, 633–667.

Omlin, M., Reichert, P. & Forster, R. (2001). Biogeochemical model of Lake Zurich: model equations and results. *Ecol. Model.*, 141, 77–103.

Otto, S., Rall, B.C. & Brose, U. (2007). Allometric degree distributions facilitate food-web stability. *Nature*, 450, 1226–1229.

Pauly, D., Christensen, V. & Walters, C. (2000). Ecopath, Ecosim, and Ecospace as tools for evaluating ecosystem impact of fisheries. *ICES J. Mar. Sci.*, 57, 697–706.

Ricklefs, R.E. (2008). Disintegration of the ecological community. *Am. Nat.*, 172, 741–750.

Rosenzweig, M.L. & MacArthur, R.H. (1963). Graphical representation and stability conditions of predator–prey interactions. *Am. Nat.*, 97, 209.

Sheldon, R.W., Prakash, A. & Sutcliffe, W.H. (1972). The size distribution of particles in the ocean. *Limnol. Oceanogr.*, 17, 327–340.

Shertzer, K.W., Ellner, S.P., Fussmann, G.F. & Hairston, N.G. (2002). Predator-prey cycles in an aquatic microcosm: testing hypotheses of mechanism. *J. Anim. Ecol.*, 71, 802–815.

Sommer, U., Gliwicz, Z.M., Lampert, W. & Duncan, A. (1986). The PEG-model of seasonal succession of planktonic events in fresh waters. *Arch. Hydrobiol.*, 106, 433–471.

Tirok, K. & Gaedke, U. (2007a). Regulation of planktonic ciliate dynamics and functional composition during spring in Lake Constance. *Aquat. Microb. Ecol.*, 49, 87–100.

Tirok, K. & Gaedke, U. (2007b). The effect of irradiance, vertical mixing and temperature on spring phytoplankton dynamics under climate change: long-term observations and model analysis. *Oecologia*, 150, 625–642.

Tirok, K. & Gaedke, U. (2010). Internally driven alternation of functional traits in a multispecies predator-prey system. *Ecology*, 91, 1748–1762.

Tirok, K., Bauer, B., Wirtz, K. & Gaedke, U. (2011). Predator–prey dynamics driven by feedback between functionally diverse trophic levels. *PLoS ONE*, 6, e27357.

Williams, R.J. (2008). Effects of network and dynamical model structure on species persistence in large model food webs. *Theor. Ecol.*, 1, 141–151.

Williams, R.J. & Martinez, N.D. (2000). Simple rules yield complex food webs. *Nature*, 404, 180–183.

Williams, R.J. & Martinez, N.D. (2004). Stabilization of chaotic and non-permanent food-web dynamics. *Eur. Phys. J. B*, 38, 297–303.

Williams, R.J. & Martinez, N.D. (2008). Success and its limits among structural models of complex food webs. *J. Anim. Ecol.*, 77, 512–519.

Williams, R.J., Brose, U. & Martinez, N.D.. (2007). Homage to Yodzis and Innes 1992: scaling up feeding-based population dynamics to complex ecological networks. In: *From Energetics to Ecosystems: The Dynamics and Structure of Ecological Systems* (eds Rooney, N., McCann, K.S. & Noakes, D.L.G.). Springer, The Netherlands, pp. 37–52.

Yodzis, P. & Innes, S. (1992). Body size and consumer-resource dynamics. *Am. Nat.*, 139, 1151–1175.

Yoon, I., Williams, R.J., Levine, E., Yoon, S., Dunne, J.A. & Martinez, N.D. (2004). Webs on the Web (WoW): 3D visualization of ecological networks on the WWW for collaborative research and education. *Proc. IS&T/SPIE Symp. on Electronic Imaging, Visualization and Data Analysis*, 5295, 124–132.

Yoshida, T., Ellner, S.P., Jones, L.E., Bohannan, B.J., Lenski, R.E. & Hairston, N.G. (2007). Cryptic population dynamics: rapid evolution masks trophic interactions. *PLoS Biol.*, 5, 1868–1879.

SUPPORTING INFORMATION

Additional Supporting Information may be downloaded via the online version of this article at Wiley Online Library (www.ecologyletters.com).

As a service to our authors and readers, this journal provides supporting information supplied by the authors. Such materials are peer-reviewed and may be re-organised for online delivery, but are not copy edited or typeset. Technical support issues arising from supporting information (other than missing files) should be addressed to the authors.

Editor, Giulio De Leo
Manuscript received 2 November 2011
First decision made 11 December 2011
Second decision made 5 March 2012
Manuscript accepted 14 March 2012